Nanomaterials: Types, Synthesis and Characterization

5

T. C. Mokhena, M. J. John, M. A. Sibeko, V. C. Agbakoba, M. J. Mochane, A. Mtibe, T. H. Mokhothu, T. S. Motsoeneng, M. M. Phiri, M. J. Phiri, P. S. Hlangothi, and T. G. Mofokeng

Abstract

Nanoparticles are generally defined as particles having one or more dimensions of sizes ranging from 1 to 100 nm. Nanoparticles can be classified into organic, inorganic and carbon-based materials. In comparison with conventional micro-size particles, nanoparticles show enhanced properties, such as high reactivity, strength, surface area, sensitivity and stability due to their nanosize. Various preparation methods, viz. physical, chemical and mechanical, have been employed to synthesize different nanoparticles. This chapter presents an overview on nanoparticles and their types, properties, synthesis methods and application in bioconversion of biomass into biofuels.

T. C. Mokhena (✉) · M. J. John · V. C. Agbakoba
Department of Chemistry, Nelson Mandela University, Port Elizabeth, South Africa

CSIR Materials Science and Manufacturing, Polymers and Composites, Port Elizabeth, South Africa

M. A. Sibeko · M. M. Phiri · M. J. Phiri · P. S. Hlangothi
Department of Chemistry, Nelson Mandela University, Port Elizabeth, South Africa

M. J. Mochane
Department of Life Sciences, Central University of Technology Free State, Bloemfontein, South Africa

A. Mtibe · T. S. Motsoeneng
CSIR Materials Science and Manufacturing, Polymers and Composites, Port Elizabeth, South Africa

T. H. Mokhothu
Department of Chemistry, Durban University of Technology, Durban, South Africa

T. G. Mofokeng
DST/CSIR National Centre for Nanostructured Materials, Council for Scientific and Industrial Research, Pretoria, South Africa

M. Srivastava et al. (eds.), *Nanomaterials in Biofuels Research*, Clean Energy Production Technologies, https://doi.org/10.1007/978-981-13-9333-4_5

Keywords
Nanoparticles · Synthesis · Characterization · Properties · Biofuel application

5.1 Introduction

Nanotechnology has been a topical subject in the academia and industrial communities for the past years (Zhang et al. 2013; Romero and Moya 2012; Margulis-Goshen and Magdassi 2012; Moreno-Vega et al. 2012). This technology offers a new dimension to a science of working and manipulating materials having a size of 100 nm or less at least in one dimension (Zhang et al. 2013). With respect to their nanosize, these materials are recognized by their unique properties, viz. physicochemical and mechanical properties such as reactivity, tenacity, elasticity, strength and excellent electrical and thermal conductivities. These nanomaterials can easily be employed in a wide range of fields including crop production, cosmetics, drug delivery, photonic crystals, analysis, food, coatings, paints, bioremediation, catalysis and material science. The nanomaterials' size, shape and morphology play a significant role on their properties; therefore, more research has been dedicated in finding means to fine-tune these properties (Romero and Moya 2012; López-Serrano et al. 2014). For example, gold (Au), platinum (Pt), silver (Ag) and palladium (Pd) nanoparticles all with a size of 20 nm have characteristic colours, i.e. wine red, yellowish-grey, black and dark black colours, respectively (Khan et al. 2017). The overall shapes can be 0D, 1D, 2D or 3D.

Nanotechnology can simply be defined as the science of designing, synthesizing and characterizing nanomaterials as well as their applications. Since the introduction of the term "nanotechnology", there has been a lot of reports based on the classification, preparation and characterization of nanomaterials. Different synthesizing routes have been developed in order to control the size, structure and morphology of the resulting nanomaterials. These include chemical vapour deposition (CVD), sol-gel technique and mechanochemical processes. The preparation route depends on the resulting nanoparticle type and properties and thus intended application. Inorganic nanoparticles such metal oxides are often produced via wet chemistry, sol-gel, chemical microemulsion, hydrothermal, solvothermal, microwave-assisted combustion, sonochemical and direct precipitation, whereas carbon-based nanomaterials are usually produced through techniques such as arc discharge (AD), laser ablation and chemical vapour deposition (CVD). In the case of graphene nanosheets, techniques such as chemical, mechanical and thermal exfoliation are used. Despite the success that has been made on the production of various nanomaterials, the use of green methods in order to produce these materials has been one of the major research activities for the past decade (Shao et al. 2018; Logeswari et al. 2015). In this case, the plant extract or natural material is either used as reducing or stabilizing agent for nanoparticle production. Chitosan and alginate were recently reported as a suitable stabilizing and reducing agent in synthesizing silver nanoparticles (AgNPs) (Shao et al. 2018; Logeswari et al. 2015; Mokhena and Luyt 2017a; Mokhena and Luyt 2017b).

Nanotechnology application in biofuel production provides very intriguing solutions to some challenges faced in this field. Nanomaterials can be used as favourable carriers to immobilize some catalyst in order to facilitate their recovery from liquid phase by filtration or centrifugation (Zhang et al. 2013). For instance, it was demonstrated that modified nanosphere silica realizes the extraction from alive microalgae without harm which avoids recultivation by sending the microalgae back for lipid accumulation (Lin et al. 2009). Moreover, nanoparticles can be used directly as heterogeneous catalysts in order to improve the biofuel conversion yields and resultant fuel quality (Wen et al. 2010). Nanoparticles such as CaO, Al_2O_3 and MgO are already being recognized as heterogeneous catalysts with conversion rate of more than 99% with less amount of oil (i.e. ˂1%) (Zhang et al. 2013; Wen et al. 2010; Venkat Reddy et al. 2006). There has been quite a lot of publications, reviews and book chapters covering the use of nanoparticles in order to facilitate the biofuel production and resultant fuel quality (Zhang et al. 2013; Lee et al. 2015). This chapter presents an overview on nanoparticles and their types, properties, synthesis methods and application in bioconversion of biomass into biofuels.

5.2 Classification

Nanoparticles can be classified either by source (natural or anthropogenic); chemical composition (organic or inorganic); synthetic route (biogenic, geogenic, anthropogenic and atmospheric); their shape, size or structure; or their applications (Romero and Moya 2012; Margulis-Goshen and Magdassi 2012; Khan et al. 2017; Cui et al. 2018). In this chapter, we reviewed the nanoparticles based on their chemical composition as discussed below. In general, the fabrication/preparation of the nanoparticles can either be "bottom-up" or "top-down" approach as schematically presented in Fig. 5.1. Bottom-up approach as reflected by its name involves building up NPs from single molecule or atom, e.g. sedimentation and reduction techniques. In this context, precursor or source is used as simple substance to synthesize NPs either by sedimentation or reduction. Examples include sol-gel, biosynthesis, spinning and pyrolysis. On the other hand, top-down approach involves breaking down bulk materials into smaller units which are further converted into suitable NPs. Examples include milling, CVD, physical vapour deposition and decomposition processes.

5.2.1 Organic Nanoparticles

Organic nanoparticles feature unique properties such as biodegradability, biocompatibility and high stability in biological fluids (Romero and Moya 2012; Margulis-Goshen and Magdassi 2012; Moreno-Vega et al. 2012). These particles are available in nature as protein aggregates, lipid bodies, milk emulsions or more complex organized structures such as viruses, etc. Organic nanoparticles have been used as a part of different industrial products, such as food (e.g. creams, chocolate and cakes) and

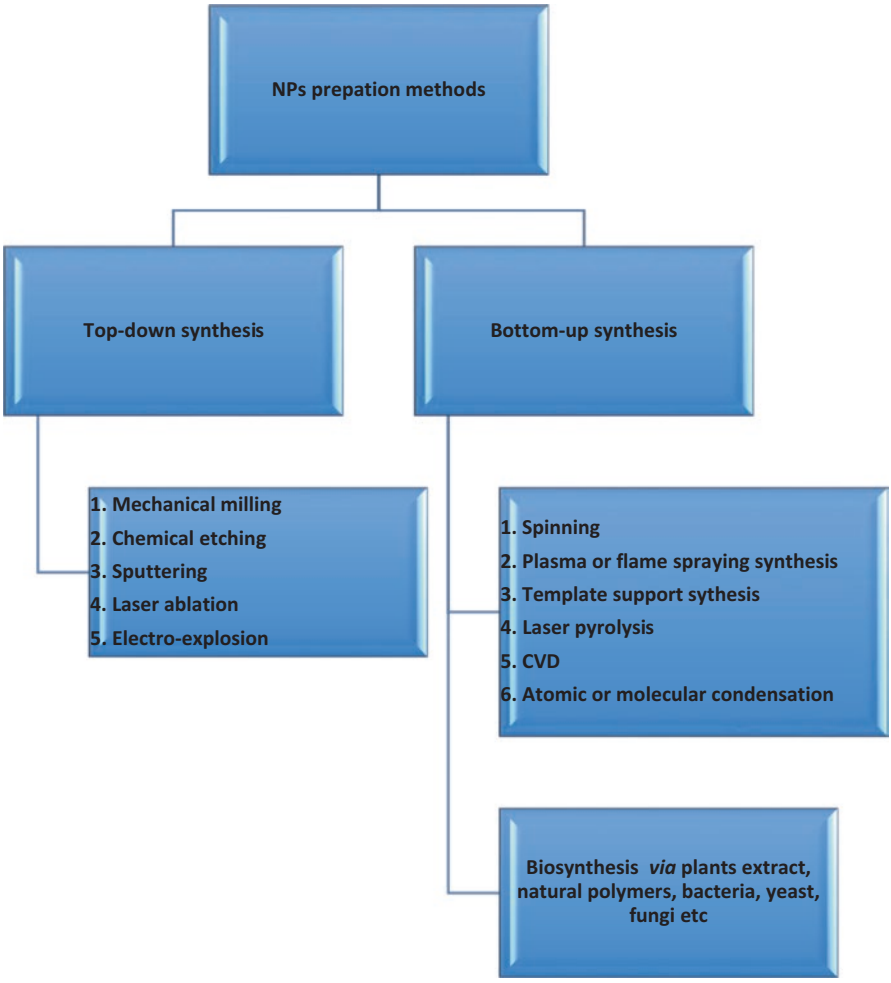

Fig. 5.1 Schematic presentation of synthetic routes for NPs

cosmetics (as nanoemulsions), and in pharmaceutical formulations (viz. liposome vectors, polymersomes and polymer-protein and polymer-drug conjugates). Organic nanoparticles are often fabricated by both "top-down" and "bottom-up" approaches as discussed in the next sections (Romero and Moya 2012; Margulis-Goshen and Magdassi 2012; Cui et al. 2018).

5.2.1.1 Synthesis of Organic Nanoparticles

The "top-down" approach such as milling, lithography and microfluidics is often used to physically reduce the size of bulk material into nanomaterials (Romero and Moya 2012; Rolland et al. 2005). Milling is the most used process especially for drug NPs made from poor water-soluble compounds. The limitations of the milling

process include unavoidable contamination of the produced NPs and their wide size distribution. Elsewhere, it was demonstrated that a wet milling process can be employed to produce particles having sizes of 230 nm from poor water-soluble drug crystals (Sigfridsson et al. 2011). The obtained NPs were chemically stable for 10 months in both room temperature and when refrigerated and physically stable (particle size) for 10 months under refrigeration and 3 years at room temperature. Microfluidic and lithography are often employed in order to gain more control over the size and the shape of the resulting NPs. A very general top-down approach, particle replication in nonwetting templates (PRINT), was used to fabricate monodisperse particles with simultaneous control over structure (i.e. shape, size and composition) and function (i.e. cargo, surface structure) by Rolland et al. (Rolland et al. 2005). They prepared monodispersed NPs of poly(ethylene glycol diacrylate), triacrylate resin, poly(lactic acid) and pyrrole having sizes below 200 nm. Considering the compatibility of PRINT with other synthetic schemes (free radical polymerization, metal-catalysed high-temperature reaction, oxidative coupling using strong acids), it demonstrated its chemical flexibility and tolerance which is important for production of NPs for various applications.

Bottom-up approach is based on building NPs through physicochemical processes, starting from single molecule or atoms (Romero and Moya 2012). It involves single atom or molecule combining via synthetic chemistry and self-organization to produce various organic nanoparticles, such as micelles, vesicles and liposomes, polymersomes, polymer conjugates, dendrimers, capsules and polymeric NPs (Romero and Moya 2012).

5.2.2 Inorganic Nanoparticles

5.2.2.1 Metal Oxide and Metallic Nanoparticles

Metal and metal oxide nanoparticles include silver, silver oxide, copper oxide, magnesium oxide, ZnO, Fe_3O_4 and many more (Jamdagni et al. 2018). Metal oxide nanoparticles feature unique characteristics such as antifungal, antimicrobial, optical absorption, large surface-to-volume ratio, semiconducting and chemical-sensing properties. In addition, their non-toxicity and biocompatibility characteristics offer them opportunity to be applied in different fields such as biomedical, food packaging, biofuel conversion and agriculture. Several researchers have investigated the small-scale production of metal and metal oxide NPs using chemical, green, physical and a combination of these methods with some showing a great potential for large-scale production (Jamdagni et al. 2018) (Table 5.1).

5.2.2.1.1 Synthesis of Metal and Metal Oxide Nanoparticles

Several methods have been applied to synthesize metal and metal oxide nanoparticles, such as physical, chemical, enzymatic and biological methods(Ahmed et al. 2017). Physical methods include plasma arcing, ball milling, thermal evaporation, spray pyrolysis, ultrathin films, pulsed laser desorption, lithographic techniques, sputter deposition, layer-by-layer growth and diffusion flame synthesis. Chemical

Table 5.1 Selected studies on the synthesis of nanoparticles and their properties

Type	Precursor	Route	Techniques	Highlights	References
AgNPs	Silver nitrate ($AgNO_3$)	Biosynthesis using chitosan as stabilizing and reducing agent	UV-vis, TEM and FTIR	The optimum preparation time for AgNPs was 12 h heating at 90 °C to obtain NPs of sizes of 5–20 nm	Mokhena and Luyt (2017a, b)
ZnNPs	Zinc acetate dehydrate ($Zn(CH_3COO)_2{\cdot}2H_2O$)	Biosynthesis using extract from *Nyctanthes arbor-tritis*	UV-vis, FTIR, XRD, DLS and TEM	NPs had size range of 12–32 nm	Jamdagni et al. (2018)
ZnNPs	$ZnCl_2$	Hydrothermal method	UV-vis, XRD, SEM, TEM, SAED	ZnO hollow spheres	Yu and Yu (2008)
TiO_2	Tetrabutyl orthotitanate ($(Ti(OC_4H_9)_4)$)	Hydrothermal method	XRD, XPS, TEM, BET	Mesoporous fluorinated anatase TiO_2 powders having primary particles of 11 ± 2 nm	Yu et al. (2009)
ZnNPs	Zinc acetate	Spray pyrolysis	XRD	Polycrystalline films having hexagonal wurtzite-type crystal structure with grain size of 20 nm	Ashour et al. (2006)
MgO	Magnesium nitrate ($mg(NO_3)_2.6H_2O$)	Spray pyrolysis	XRD, TEM, UV-vis	Crystallite size of 9 nm was obtained	Nemade (2014)
ZnNPs	ZnO powder	Chemical vapour deposition	SEM, TEM, SAED, XRD	Nanowires with diameter of 5 nm and length of 50 nm	Xiang et al. (2007)

methods include electrodeposition, sol-gel process, chemical solution deposition, chemical vapour deposition, Langmuir-Blodgett method, soft chemical method, hydrolysis, co-precipitation and wet chemical methods. One of the most widely used chemical syntheses is co-precipitation (Dobrucka and Długaszewska 2016). In this case, the metal oxide precursor is mixed with stabilizing agent to form nanoparticles. Chemical synthesis is disadvantageous because it requires hard labour and is time consuming and costly (Dobrucka and Długaszewska 2016). Moreover, the chemical used is toxic and may contaminate the resulting NPs and produces large amount of secondary wastes. In solvothermal method, two steps are involved: (i) NPs are synthesized from chemical method and (ii) then calcined at high temperatures. In this method, it is possible to control the size, shape and crystallinity of the metal oxide or metal nanoparticles by changing the experimental conditions such as temperature, reaction time, solvent type, surfactant type and precursor type.

Hydrothermal synthesis has also been utilized to fabricate metal or metal oxide nanoparticles (Yu and Yu 2008; Yu et al. 2009). Similar to solvothermal method, it involves high temperatures and pressures (in autoclave), but the solution is non-aqueous (Yu and Yu 2008). Yu and Yu (2008) synthesized hollow spheres of ZnO nanoparticles by hydrothermal approach from a mixture of sugar and $ZnCl_2$. This mixture was treated at 180 °C for 24 h and then calcined in air at 500 °C for 4 h. The average diameter of as-prepared microsphere was 10 μm (Fig. 5.2a) which drastically decreased to about 800 nm after calcination (Fig. 5.2b). The hollow spheres had shell thickness of about 60 nm (Fig. 5.2c) which were polycrystalline (inset in

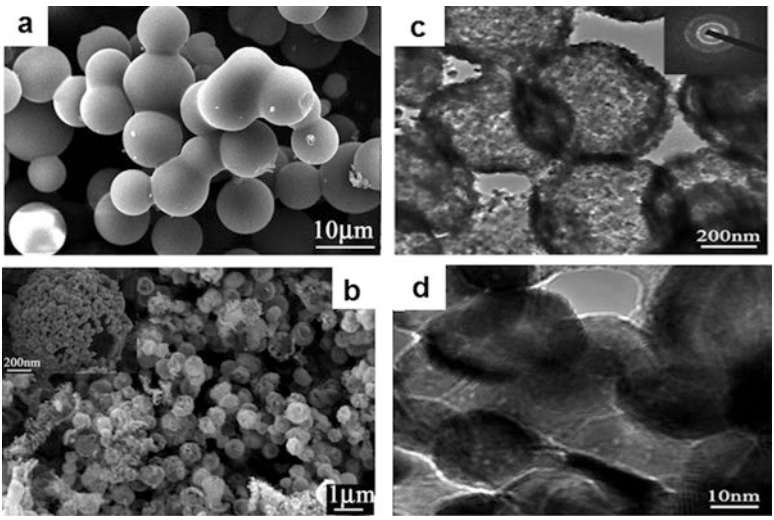

Fig. 5.2 SEM images of the ZnO hollow spheres prepared before calcination (**a**) and after calcination (**b**) at 500 °C for 4 h. TEM image (**c**), high magnification. TEM image (**d**) and SAED pattern (inset in **c**) of the ZnO hollow spheres prepared and calcined at 500 °C for 4 h. (Reprinted with permission from Yu and Yu 2008 with permission from American Chemical Society)

Fig. 5.2a). It was observed that the hollow spheres were composed of randomly aggregated nanocrystal particles with sizes of about 18 nm.

Biosynthesis is a new area of nanotechnology in which natural materials are used to synthesize different nanoparticles (Jamdagni et al. 2018; Ahmed et al. 2017; Dobrucka and Długaszewska 2016; Matinise et al. 2017). These materials can be used as either stabilizing or reducing agent or both. The economic and environmental benefit associated with this technique opens the door for future NP production especially to overcome the challenges associated with chemical and physical methods. Natural materials such as gelatine, alginate, chitosan and many more have been studied for the synthesis of metal oxide nanoparticles as depicted in Table 5.1. In general, the natural polymer or plant extracts are mixed with precursor and then heated under certain temperature and for a given period to obtain NPs (Jamdagni et al. 2018; Matinise et al. 2017). The extracts or natural polymers may act as either reducing agent or stabilizing agent or both.

Another strategy to synthesize NPs involves sol-gel technique (Tamilselvi et al. 2013). This process is divided into two reaction steps (considered as chemical method), namely, hydrolysis and condensation. Hydrolysis is when hydroxyl groups (−-OH) are produced, whereas condensation involves polycondensation of the formed hydroxyl groups and residual alkoxy groups to form a 3D network (Mtibe et al. 2018). These steps solely depend on the presence of catalyst, type and concentration as well as the ratio of water and alkoxide. The sol-gel can further be classified into (i) hydrolytic route which involves water as ligand and solvent and (ii) nonhydrolytic route which involves ethers, alcohols and ketones as oxygen donors (Mtibe et al. 2018). The sol-gel technique offers the processor the opportunity to control the properties of the resulting nanoparticles through large number of parameters such as pH, temperature, hydrolysis and condensation rate of the metal oxide precursor, the nature and concentration of anions, the method of mixing and the mixing rate (Mtibe et al. 2018). The advantage of this technique includes a control on particle-size distribution, choice of precursor, high yield and low overall production cost (Tamilselvi et al. 2013).

Chemical vapour deposition (CVD) is known as a parent to a family of processes used to coat almost any metallic or ceramic compound, including elements, metals and their alloys and intermetallic compounds (Guo et al. 2011; Carlsson and Martin 2010; Wang 2011). It involves a solid material being deposited from a vapour by a chemical reaction occurring in the vicinity of a normally heated substrate. The resulting solid materials include thin films, powder or single crystal. It is recognized that by varying the experimental conditions, substrate material, substrate temperature and composition of the reaction gas mixture, total pressure gas flows' different materials having a wide range of physical, tribological and chemical properties can be produced (Guo et al. 2011; Carlsson and Martin 2010; Wang 2011). The CVD process includes chemical vapour deposition, metal-organic chemical vapour deposition, low-pressure chemical vapour deposition, laser chemical vapour deposition, photochemical vapour deposition, chemical vapour infiltration, chemical beam epitaxy, plasma-assisted chemical vapour deposition and plasma-enhanced chemical vapour deposition. The most used methods are thermal chemical vapour deposition,

plasma-enhanced chemical vapour deposition and laser chemical vapour deposition (Carlsson and Martin 2010). This technique has been employed in the production of oxides, nitride and carbide nanopowders.

Spray pyrolysis involves the particle formation through atomization of liquid feed in a spray nozzle, combustion of the precursor, evaporation and decomposition of the metal precursor molecules and then nucleation of the particle clusters and growth of particles by condensation and coagulation (Nemade 2014; Meland et al. 2006; Patil 1999). Flame pyrolysis can be utilized to produce metal oxide nanoparticles with large surface through flame conditions and the burner design. The properties of the resulting NPs can further be modified by changing the conditions during the synthesis. For instance, the rutile phase appeared when the preparation temperature was increased and surpassed anatase when temperature was above 1000 °C; however, below 800 °C rutile was not observed (Seo et al. 2006). In addition, the average sizes of the crystallite increased with an increase in preparation temperature. This method is capable of yielding high-purity homogeneous samples, and up-scaling is possible (Meland et al. 2006).

5.2.3 Carbon-Based

5.2.3.1 Graphene

Graphene is recognized as a monolayer of graphite consisting of a honeycomb network of sp^2-hybridized carbon atoms (Goriparti et al. 2014; Kucinskis et al. 2013). The carbons are bonded into 2D sheets having nanometre thickness (single-atom thickness). It has distinctive properties which include high electrical conductivity, good mechanical properties, large surface area and high values of charge mobility, hence receiving unprecedented interest from various fields such as chemical, physical, biological and engineering sciences (Goriparti et al. 2014; Kucinskis et al. 2013). Graphene can be fabricated using various methods, such as micromechanical exfoliation of highly oriented pyrolytic graphite with or without previous processing surface, epitaxial growth, chemical vapour deposition (CVD) and reduction of graphene oxide (GO) (Goriparti et al. 2014; Kucinskis et al. 2013). The most preferable route is the reduction of GO because this process is the most suitable for large-scale production.

5.2.3.1.1 Synthesis of Graphene

Natural graphite also known as expandable graphite is one of the carbon-based material used to produce graphene by various exfoliation processes such as mechanical, chemical or electrochemical and thermal exfoliation techniques. These techniques can be used alone or in combination in order to produce graphene of high-quality and fine-tuned morphology or structure. Mechanical exfoliation or micromechanical cleavage is the most used method to obtain graphene layers. This is the first method which was reported for graphene layers' production using scotch/adhesive tape by repeated peeling of graphite crystal (Novoselov et al. 2004). Another mechanical technique involves rubbing multilayer graphene against a flat

surface to obtain a single graphene layer (Mtibe et al. 2018; Bonaccorso et al. 2012). The use of atomic force microscopy (AFM) tip by gluing graphite on it and scratching on Si substrate also offers the production of 2D graphene layers (Bonaccorso et al. 2012). This method, however, offers minimal control over separation and number of resulting graphene layers; hence, it is still difficult for most of these mechanical techniques to be realized as scalable and cost-effective (Mtibe et al. 2018; Bonaccorso et al. 2012).

Chemical exfoliation involves the use of strong oxidants and acids to oxidize graphite through Hummers, Staudenmaier and Brodie methods or by electrochemical oxidative exfoliation of bulk natural graphite (expandable graphite) to yield expanded graphite (EG) or graphite oxide (GO) (Mtibe et al. 2018; Cooper et al. 2014; Zhong and Swager 2012). The oxygen functionality on GO facilitates the dispersion of the sheets in aqueous and organic solvents, however at the expense of electronic conductivity of graphene. The disadvantage of chemical process is the use of harsh chemicals, which are not environment friendly and not easy to handle, and the long production periods associated with this process (Mtibe et al. 2018; Cooper et al. 2014; Zhong and Swager 2012). Thermal exfoliation involves the exposure of expandable graphite to rapid heat, and thus, forcing the graphite sheets apart results in an enormous increase in volume and high surface area material with low bulk density. The chemical and thermal processes can be used together to afford maximum exfoliation of the expandable graphite.

X-ray diffraction (XRD), Raman spectroscopy, transmission electron microscopy (TEM) and scanning electron microscopy (SEM) are usually used to establish the extent of exfoliation or the properties of the resulting graphene layer. Among these techniques, TEM is the most reliable technique to elucidate the properties of resulting material. For instance, the difference between the products obtained from graphite electrode using ionic liquid-assisted electrochemical exfoliation was reported by Lu et al. (2009). They studied time dependence of products exfoliated from graphite in three different stages in the electrochemical exfoliation (Fig. 5.3) using high-resolution TEM. Each stage resulted in different products as reflected by colour change, and their structure is analysed by TEM. Stage I led to hexagonal-shaped water-soluble and fluorescent carbon nanocrystals sized 8–10 nm (Fig. 5.4a). The nanocrystals had a lattice spacing of 0.21–0.25 nm comparable to the (100) facet of graphite (Fig. 5.4b). In stage II, fluorescent nanoribbons of 10 nm × (60 ± 20) nm size with flat rectangular edges with some graphene were obtained. The nanoribbons had a lattice distance of 0.34 nm that corresponds to the (002) plane of graphite (Fig. 5.4c, d), while ultrathin graphene sheets (200 nm × 500 nm) were obtained as shown in Fig. 5.4e, f.

5.2.3.2 Carbon Nanotubes (CNTs)

Carbon nanotube features unique characteristics such as high electrical and thermal conductivities and extremely large surface because of their 1D tubular structure (Goriparti et al. 2014; Liu et al. 2012; Mubarak et al. 2014; Fang et al. 2016). CNTs are recognized as cylinders consisting of rolled-up graphene sheets with hollow central core having diameters on nanometer scale and end caps with a hemisphere

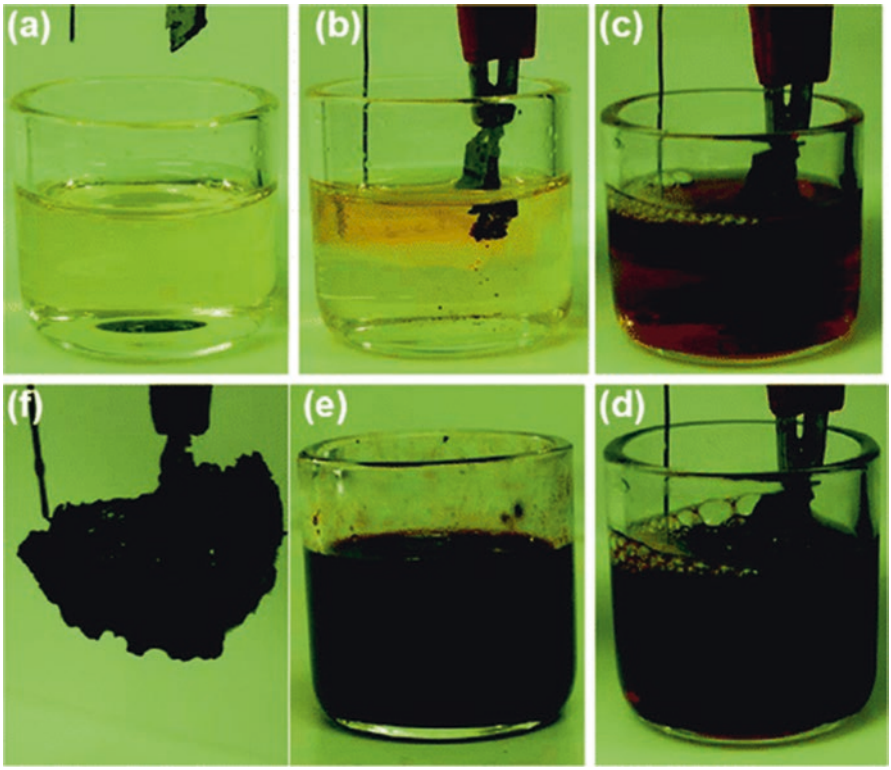

Fig. 5.3 Time evolution of IL electrolyte and highly oriented pyrolytic graphite (HOPG) anode during exfoliation in 60 wt % water/[BMIm][BF_4] electrolyte. Stages I, II and III are shown correspondingly in panels b, c and d. Heavily expanded HOPG is obtained in panel f. (Copied from Lu et al. 2009 with permission from American Chemical Society)

of fullerene structure. They are categorized into single-walled CNTs (SWCNTs) and multi-walled CNTs (MWCNTs) based on the number of graphene layers. As reflected by their names, SWCNTs consist of a single graphene layer, while MWCNTs consist of two or more graphene layers with van der Waals forces between these layers (Goriparti et al. 2014; Liu et al. 2012). In general, CNTs are often synthesized using various techniques, such as arc discharge (Mubarak et al. 2014; Fang et al. 2016; Zhao et al. 2006), laser ablation (Choi et al. 2016; Bota et al. 2015; Vander Wal et al. 2003), gas-phase catalytic growth from carbon monoxide and chemical vapour deposition (CVD) from hydrocarbons. Among these methods, gas-phase methods such as CVD have a potential for large-scale production at fairly low cost. Chemical bonding of CNTs consists of entirely sp^2 carbon-carbon bonds which are stronger than the sp^3 bonds found in diamond, thus providing CNTs with such remarkable mechanical properties (Young's modulus of 1.2 TPa and tensile strength of 50–200 GPa) (Goriparti et al. 2014; Liu et al. 2012).

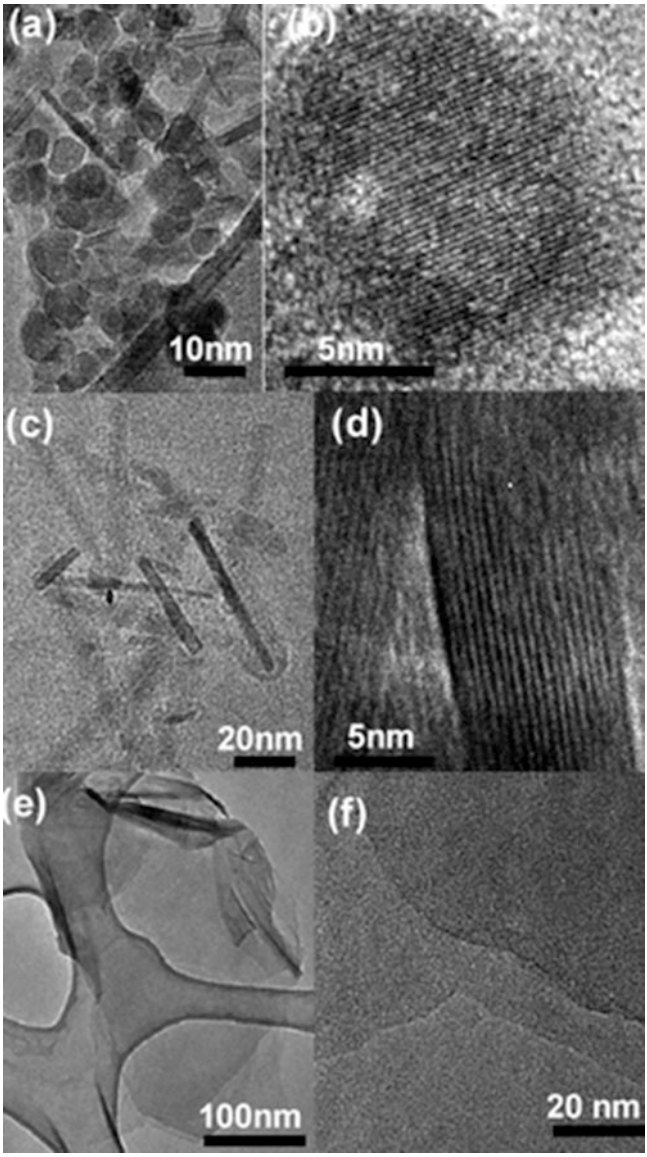

Fig. 5.4 TEM images of carbon nanoparticles (**a**, **b**), carbon nanoribbons (**c**, **d**) and graphene sheets (**e**, **f**) produced in the one-pot electrochemical exfoliation (Reprinted from Lu et al. 2009 with permission from American Chemical Society)

5.2.3.3 Synthesis of CNTs

Different types of CNTs can be produced using various techniques which include electric AD, laser ablation and CVD. These techniques require carbon source, catalyst and energy to produce CNTs. In the case of electric AD method, electric

discharge is used as energy source with electric current ranging from 40 to 125 A and potential difference ranging from 20 to 50 V (Fang et al. 2016; Zhao et al. 2006; Kim and Kim 2006; Berkmans et al. 2015; Maria and Mieno 2015; Su et al. 2011, 2014). The graphite electrodes are placed close to each other (1 mm) under inert atmosphere (i.e. at a pressure of 500 Torr) (Mtibe et al. 2018). Moreover, the metal catalyst such as cobalt, nickel, yttrium or iron and high temperatures (2000–3000 °C) are required in order to evaporate the carbons from the electrodes (Mubarak et al. 2014; Fang et al. 2016; Zhao et al. 2012). The evaporated carbon is then condensed in the cathode to form CNTs with diameters of 0.6–1.2 nm. The processors can vary experimental parameters such as metal catalyst concentration, electrode gap, current flow rate, temperature distribution gas type and gas pressure in order to afford the production of either MWCNTs or SWNTs (Mubarak et al. 2014; Fang et al. 2016; Zhao et al. 2006; Kim and Kim 2006; Berkmans et al. 2015; Maria and Mieno 2015; Su et al. 2011). By varying the ratio of catalyst (yttrium and nickel) and carbon source concentration, different carbon-based materials were obtained (Berkmans et al. 2015). It was revealed that a combination of SWCNT having a diameter of ~5.7 nm and single-walled carbon nanohorn (SWCNH) bundles sized about 25 nm can be produced using arc discharge technique in an open air atmosphere which makes this method cheaper and effective for hybrid carbon materials. However, low yields and the quality of CNTs produced via this method limit its industrial production (Mubarak et al. 2014; Berkmans et al. 2015; Su et al. 2011, 2014). The effect of the ratio of gases, viz. carbon monoxide (CO) and helium, and pressure was investigated by Su et al. (Su et al. 2011). It was reported that impurities increased with an increase in the concentration of CO in the gas mixture; however, the gas pressure $>$ 4 kPa can result in smaller diameters. Laser ablation uses the same principle as AD but uses laser pulses as source rather than heat (Choi et al. 2016; Bota et al. 2015; Vander Wal et al. 2003; Chrzanowska et al. 2015). It is recognized that the yield and quality of the resulting CNTs depend on the laser power, catalyst and temperature (Bota et al. 2015; Chrzanowska et al. 2015). In a similar manner, this technique suffers from low yield and low quality of resulting material and requires high level of purification process (Bota et al. 2015; Chrzanowska et al. 2015).

CVD merits special interest due to its capability for large-scale production of high-quality and well-oriented CNTs (Ji et al. 2017; Marchand et al. 2013; Meysami et al. 2013a). In this case, the carbon sources are the hydrocarbons methane, ethylene and benzene and metal catalysts Ni, Co and Fe. Furthermore, high temperature is also required for the production of CNTs. In this regard, the hydrocarbons' catalytic decomposition on monolayer metal catalyst is carried out at temperatures 700–900 °C to form CNTs. The quality of CNTs, yield and structure can be improved by using a single or more metal catalyst. Quite a lot of studies have been carried out to modify CVD in order to improve growth rate, quality and yield as well as to produce different types of CNTs. These modified systems include aerosol-assisted chemical vapour deposition (AACVD) (Marchand et al. 2013; Meysami et al. 2013a, b, 2015), plasma-enhanced chemical vapour deposition (PECVD) (Ji et al. 2017), hydrogen-free spray pyrolysis CVD (Ionescu et al. 2011), catalytic CVD (Almkhelfe et al. 2017; Maruyama et al. 2016; Miura et al. 2018), low-temperature CVD (Maruyama et al. 2002) and alcohol combustion CVD (Hou et al. 2017).

5.3 Characterization

Chemical composition, structure, size and shape play significant role on the properties of resulting NPs; thus, several analytical techniques were utilized to characterize these properties (Hoo et al. 2008).

5.3.1 Size Determination

NPs are often characterized based on their size, morphology and surface charge using various microscopic techniques, such as scanning electron microscopy (SEM), transmission electron microscopy (TEM), scanning tunnelling microscopy (STM) and atomic force microscopy (AFM) (Hoo et al. 2008; Binnig and Rohrer 1983). TEM and SEM are essential for providing information based on the NPs' surface, crystal structure, elemental composition, size and shape. It is recognized that the treatment of the sample before the analysis (coating, drying, staining, etc.) and vacuum conditions in the chamber may result in imaging artefacts. Field emission scanning electron microscopy (FESEM) can overcome these limitations by imaging samples which are not pretreated; however, in most cases, the samples are still treated. On the other hand, AFM provides information based on the size, morphology and surface texture and roughness (Hoo et al. 2008). However, AFM may overestimate the dimensions of the NPs especially when the geometry of the tip is larger than the NPs themselves. In the case of STM, atoms and molecules made up of NPs can be identified by alternating the environment that the specimen is observed, such as vacuum, liquid environment or gaseous environment (Binnig and Rohrer 1983).

Light scattering techniques (e.g. dynamic light scattering (DLS)) are mostly employed to establish the NPs' size (Hoo et al. 2008; Glatter 2018). Dynamic light scattering (DLS), also known as photon correlation spectroscopy, is the most used technique to determine the size of the particle in colloidal suspensions. The suspended particles undergo random Brownian motion; hence, the light scattered off the particles in suspension renders calculation of particle size. The calculation is obtained from analysing fluctuation intensities of the light scattered by the particles during irradiation by a laser beam (Glatter 2018; Ramos 2017).

X-ray-based methods include X-ray absorption (XAS), X-ray fluorescence (XRF), X-ray photoelectron spectroscopy (XPS), energy-dispersive X-ray spectroscopy (EDS), small-angle X-ray scattering (SAXS) and X-ray diffraction (XRD) (Balasubramanian et al. 2014; Dao et al. 2015). These techniques are often used to provide information about surface properties and coatings, crystallographic structure, bonding environment or elemental composition. EDS and XPS are usually combined with either SEM or TEM to elemental assessment and quantitative analysis (Dao et al. 2015). X-ray absorption is used to characterize unoccupied electronic states, the chemical composition and the bonding environment in NPs (Balasubramanian et al. 2014; Dao et al. 2015; Mottana 2014). XRD is used to

establish the crystal phase and crystallinity of the NPs (Balasubramanian et al. 2014). The comparison between patterns of the as-synthesized nanoparticles with the standard (JCPDS data) gives information based on the structure and properties of the resulting NPs (Balasubramanian et al. 2014). Spectroscopic techniques are used in NPs with plasmon resonance by collective oscillations of their conduction band electrons in response to electromagnetic waves (Dutta and Ganguly 2012; Begum et al. 2018; Okitsu 2013). UV-visible is utilized to characterize the properties of metal NPs especially the size and shape as well as surface property in the case of functionalized NPs (Begum et al. 2018; Okitsu 2013). This results from plasmonic NPs absorbing radiations of visible to near-infrared region (NIR) depending on their size and shape. This character could be related to collective oscillation of surface electrons of nanoparticles and known as surface plasmon resonance (SPR) (Begum et al. 2018; Okitsu 2013). Because of the SPR property of the nanoparticles, dispersed plasmonic NPs in suspension give one or more peaks that can be used to extract valuable information with regard to the shape, size and size distribution of the nanoparticles (Begum et al. 2018; Okitsu 2013).

Nanoparticle tracking analysis (NTA) is one of commonly used systems for particles of sizes below ~20–1000 nm, with the lower detection limit being dependent on the refractive index of the NPs (van der Pol et al. 2014; Zhou et al. 2015; James and Driskell 2013). It uses a highly sensitive CCD video camera to capture scattered light from each NPs and track the Brownian motion of individual NPs to yield independent size measurements (James and Driskell 2013). Yet another technique is hyperspectral imaging which relies on scattering the obliquely incident visible and near-infrared light in an enhanced dark field. It provides information based on spatial distribution and spectral characteristics depending on NP type, at a sensitivity of a single nanoparticle (size ˂10 nm) (Pena et al. 2016; Badireddy et al. 2012).

5.3.2 Quantification

NP quantification is another important step to understand the fate, behaviour and occurrence of NPS in different environments. Different sensitive analytical techniques have been used to detect and characterize nanoparticles as discussed in the next section.

ICP spectrometry is commonly employed during NP synthesis because it is capable of determining the total element concentration of the colloidal solution (Scheffer et al. 2008). Nowadays, it has been further extended to the size characterization of NPs. ICP mass spectroscopy (ICP-MS) was recently used to establish the size distribution of nanoparticles. In this regard, the determination of discrete ion clouds generated from the atomization of a single nanoparticle in the plasma causes an intensity signal at the detector associated with the size of the particle (Scheffer et al. 2008; Degueldre et al. 2004; Degueldre and Favarger 2004). Single-particle ICP (SP-ICP) is one of the analytical techniques used to determine NP concentration, size and size distribution. It measures the intensity signal produced after ionization of an individual particle rather than a continuous flow of ions reaching the plasma

(de la Calle et al. 2017). ICP optical emission spectroscopy (ICP-EOS) has been also utilized for NP analysis (Scheffer et al. 2008; Fischer et al. 2007).

Liquid chromatography mass spectroscopy (LC-MS) is commonly used to analyse fullerenes in environmental matrices (Chen et al. 2008a). Since this technique relies on the rate at which the NPs elute from the stationery phase over a mobile phase gradient, the extraction of C60 has been exploited by its solubility in toluene (Chen et al. 2008a).

Fourier transform infrared (FTIR) and Raman spectroscopy are also used for identification of NPs. The most important range for NPs is the fingerprint region which provides signature information of the sample. Surface-enhanced Raman spectroscopy (SERS) is considered the new innovative method due to its signal-enhanced capability via SPR phenomenon (Muehlethaler et al. 2015; Ma et al. 2011).

5.4 Applications of the Nanoparticles in Biofuels

Nanomaterials can be employed in biodiesel production from biomass as substrate for lipid accumulation, lipid extraction and transesterification process as either catalyst or catalyst support. Due to their high surface area, NPs have been applied as immobilizing agent for lipids; thus, they can be easily recovered from liquid phase by either filtration or centrifugation. Since organic solvents such as hexane and methanol were mainly used in lipid extraction due to their strong affinity towards lipids, immobilization of organic solvent-like chemical onto NPs provides easy recovery and extraction of the lipids. Elsewhere, it was demonstrated that the modified nanosilica afforded the extraction of alive algae which can be sent back for further lipid accumulation again (Lin et al. 2009). Some studies also revealed that NPs enhance the growth of microalgae which improves lipid accumulation (Gao et al. 2010). However, selection of the NPs has to be carefully considered in order to avoid any negative effect on the microbes (Jin et al. 2007; Magrez et al. 2006; Williams et al. 2006).

Transesterification is one of the most reliable and simple technologies applied in biodiesel production (Lee et al. 2015). In this context, various oils from different sources such as animal, plant or oleaginous microorganisms react with alcohol to produce fatty acid methyl esters (FAMEs or biodiesel) (Lee et al. 2015). There are two conditions in which the reaction takes place, viz. either severe high temperatures and pressures or mild conditions at the presence of catalyst. In the latter, acids (H_2SO_4 and HCl) and base (NaOH and KOH) are often employed as catalyst for biodiesel production in the lab and industrial scale, respectively (Xu et al. 2006; Vicente et al. 2009; Ullah et al. 2009). The corrosiveness of the acids and soap formation for base catalyst opened door for enzymatic biocatalyst lipase which is environmentally friendly and efficient (Vicente et al. 2009; Ullah et al. 2009). However, the cost associated with the use of this enzymatic biocatalyst has been recognized as the major limitation that hurdles its success (Du et al. 2004; Pizarro and Park 2003; Noureddini et al. 2005). Different propositions have been made to reduce the overall

cost, such as reducing lipase production cost, enhancing its efficiency and reusing it for more than once. The latter has been considered as a feasible route to reduce the overall cost. In this regard, lipase has been immobilized on different carriers, which include fibre cloth, acrylic resin, silica gel, hydrotalcite and micro- and macroporous materials (Noureddini et al. 2005; Yang et al. 2006; Bai et al. 2006). In recent years, nanomaterials received tremendous interest due to their unique attributes such as large surface-to-volume ratio which can provide enormous surface area for lipase immobilization. Different nanomaterials were reported to be employed for lipase immobilization and had the capability of retaining the enzyme and improving its efficiency, selectivity and stability as summarized in Table 5.2.

It was demonstrated that the activity of the lipase immobilized onto nanosized silica was 93% after 7 months of storage as compared to 40% activity for free lipase (Kwon et al. 2007). Elsewhere, the activity was further enhanced by immobilizing lipase onto functionalized zirconia (~214%) and remained high as initially after reusing for eight times (Chen et al. 2008b). Recent study by Li et al. (Li et al. 2018) also demonstrated that other nanoparticles such as carbon nitride can also be utilized for lipase immobilization. Carbon nitride (C_3N_4) as one of the types of two-dimensional nanomaterials has the capability of immobilizing lipase to improve its efficiency. It was reported that nanosheets for immobilization of lipase exhibited satisfactory enzyme loading (44.76 mg/g), pH flexibility, thermostability (after 180 min at 50 °C, 67% of the initial activity remained) and recyclability (after 10 runs, 72% of the initial activity). The concern with regard to immobilization of biocatalyst onto nanomaterials is the recovery of these materials which can end up being cumbersome. In some studies, centrifugation has been used as a recovery technique; however, it consumes a lot of energy and time. In order to easily recover both nanomaterials and immobilized biocatalyst, the use of magnetic nanomaterials has been a major subject in research in the past decades (Tsang et al. 2006; Konwarh et al. 2009; Dyal et al. 2003; Solanki and Gupta 2011; Amirkhani et al. 2016; Netto et al. 2009; Xie and Ma 2009). The magnetic nanoparticles can be easily recovered by using external magnet, thus improving biocatalyst recovery and reusability. However, the aggregation and the nature of chemical activity of magnetic nanoparticles have been the major drawbacks (Amirkhani et al. 2016). One of the proposed methods in order to solve these problems involves coating the magnetic NPs with inorganic layers such as carbon and silica (Amirkhani et al. 2016; Lu et al. 2007; Horak et al. 2007). Moghaddas and co-workers synthesized magnetic silica aerogel support by iron oxide nanoparticles and sodium silicate precursors in a sol-gel process followed by chemical modification and ambient pressure drying (Amirkhani et al. 2016). A maximum adsorption capacity of lipase through physical adsorption was about 81.9 mg/g.

Apart from enzymatic catalyst, heterogeneous catalysts (viz. calcined Li-CaO, Mg-Al hydrotalcites, calcium oxides, magnesia-rich magnesium aluminate spinel, Mg/Zr), which are solid acid or base, have been investigated in biofuel production (Wen et al. 2010; Venkat Reddy et al. 2006; Wang et al. 2009; Sree et al. 2009). Among these, nanocatalyst renders high catalytic efficiency and eases separation from products. Biofuel production through transesterification using nanocatalyst

Table 5.2 Selected studies on the immobilization of lipase

Lipase source	NP type	Synthesizing route and highlights	Activity remaining (%)	Reusability	References
Candida rugosa	MWCNTs	MWCNTs were commercially procured having diameters of 30 ± 5 nm	97	–	Shah et al. (2007)
Candida rugosa	Fe_3O_4	Co-precipitation method to obtain NPs having sizes of 10 ± 2 nm	80	4	Solanki and Gupta (2011)
Candida rugosa	ZrO_2	Chemical method followed by calcination to obtain ZrO_2 nanoparticles having diameter of ~20 nm	214	8	Chen et al. (2008b)
Candida rugosa	Carbon nitride (C_3N_4)	Thermal exfoliation (oxidation) to obtain 2D graphene-like nanosheets	~100	10	Li et al. (2018)
Candida rugosa	γ-Fe_3O_4	Sonication of Fe(CO) in decalin followed by annealing to obtain NPs of average size of 20 ± 10 nm	˂100	–	Dyal et al. (2003)
Candida antarctica	Fe_3O_4	Co-precipitation resulted in nearly cubic particles of sizes ranging from 5 to 10 nm	200	4	Netto et al. (2009)
Thermomyces lanuginosus	SiO_2	Sol-gel process resulted in mesoporous structure having a pore size of 15 nm satisfying lipase-chitosan conjugation	93	–	Kwon et al. (2007)
Candida antarctica	Fe_3O_4	Co-precipitation to produce almost spherical NPs having diameters of ~11.2 nm	70	4	Xie and Ma (2009)

from various oils, which include plant oils and waste oils from selected studies, is summarized in Table 5.3. It is recognized that the required nanocatalyst is 30% of that of conventional catalyst to obtain similar reaction conditions. In addition, the reaction was found to be not dependent on moisture and the free fatty acid content (Venkat Reddy et al. 2006; Boz et al. 2009).

Table 5.3 Selected studies on heterogeneous nanocatalysts

Catalyst	Size and synthesizing route	Oil type	Catalyst:oil ratio (%w/w)	Reaction time (hours)	Yield (%)	References
MWCNTs	Commercially procured and impregnated with KOH and calcined	Canola	12	4	94.2	Omraei et al. (2013)
CaO-NaY-Fe3O4	Grind and then calcined resulted in NPs of average particle size of 200–500 nm with surface area of 359.42 m^2/g	Canola	–	4	95.37	Firouzjaee and Taghizadeh (2017)
CaO-AuNPs	Impregnation by deposition of AuNPs onto CaO	Sunflower	–	3	94	Bet-Moushoul et al. (2016)
TiO2-ZnO	Combustion resulted in spherical (34.2 nm) particles	Palm	–	5	92	Madhuvilakku and Piraman (2013)
CaO	Commercially procured NPs with diameters of ˃160 nm	Soybean	16	6	93.5	Luz Martínez et al. (2010)
CaO	Commercially procured with size ranging from 20 to 40 nm	Poultry oil	0.6	12	99	Venkat Reddy et al. (2006)
$Cs_2Mg(CO_3)_2$	Co-precipitation to yield NPs with crystallite size of 17.5 ± 5.3 nm and surface area of 70 m^2/g	Butter	–	3	100	(Montero et al. 2010)
KF/Al_2O_3	Commercial procured	Soybean	3	8	99.84	Boz et al. (2009)
KF/CaO-MgO	Co-precipitation resulted in mesoporous structure with pore size of about 34 nm and the grain size in the range of 100–300 nm	Rapeseed	3	3	95	Wang et al. (2009)
KF/CaO-Fe3O4	Co-precipitation followed by impregnation resulted in NPs having average diameter of 50 nm and surface area of 20.8 m^2/g	Stillingia	4	3	95	Hu et al. (2011)
$K_2O/\gamma\text{-}Al_2O_3$	Grinding calcination method to afford spherical NPs of about 50 nm	Rapeseed	3	3	94	Han and Guan (2009)

(continued)

Table 5.3 (continued)

Catalyst	Size and synthesizing route	Oil type	Catalyst:oil ratio (%w/w)	Reaction time (hours)	Yield (%)	References
Li-CaO	Impregnation method afforded a mixture of rod-shaped and hexagonal particles having sizes ranging from 50 to 70 nm	Karanja and jatropha	5	1	100	Kaur and Ali (2011)
MgO	Hydrolysis followed by supercritical solvent removal and then dehydrated to form monocrystalline particles of 1–3 nm with lattice spacing of 2.1 Å and surface area of 435 m^2/g	Sunflower and rapeseed	1.5	6	90	Verziu et al. (2008)
MgO	Decomposition of $mg(OH)_2$	Palm	0.5	4	51.3	Yacob et al. (2009)
MgO	Commercially procured having average of 60 nm	Soybean	2	17	99	Wang and Yang (2007)

5.5 Conclusion and Future Remarks

In this chapter, different fabrication methods for various nanomaterials and their characterization as well as classification were presented. It can be concluded that nanoparticles received tremendous interest towards biofuel applications due to their inherited properties, such as particle size, larger surface area, tuneable porosity, crystallinity, shape, compositions and many more. A wide variety of methods, such as microscopic, X-ray-based, light-scattering, spectroscopic and other methods, have been employed to establish these properties because they are of significance with regard to their application. From microscopic viewpoint, TEM is the most reliable technique to provide information on the size distribution and shape of nanoparticles, whereas other quantification methods can also be used to complement TEM especially towards the intended application.

Besides the fact that the utilization of the nanomaterials for advancement of biofuel production is being in its infancy, there has been progress on applying nanomaterials instead of organic solvent with regard to safety and health issues. In addition, nanomaterials can enhance lipid production (by providing stress on biomass) and lipid extraction (even without harming microalgae) and can be used as biocatalyst carriers and/or as heterogeneous catalyst in oil transesterification to biodiesel (Zhang et al. 2013). Further studies are, however, required to further our understanding with regard to cost-effectiveness recycling and impact of these NPs on the environment in order to avoid possible negative consequences on human and other organism.

Acknowledgements The authors would like to thank the financial support from the National Research Funding (NRF) and Department of Science and Technology (DST) Biorefinery Program in South Africa.

References

Ahmed S, Annu CSA, Ikram S (2017) A review on biogenic synthesis of ZnO nanoparticles using plant extracts and microbes: a prospect towards green chemistry. J Photochem Photobiol B Biol 166:272–284. https://doi.org/10.1016/j.jphotobiol.2016.12.011

Almkhelfe H, Li X, Rao R, Amama PB (2017) Catalytic CVD growth of millimeter-tall single-wall carbon nanotube carpets using industrial gaseous waste as a feedstock. Carbon 116:181–190

Amirkhani L, Moghaddas J, Jafarizadeh-Malmiri H (2016) *Candida rugosa* lipase immobilization on magnetic silica aerogel nanodispersion. RSC Adv 6(15):12676–12687

Ashour A, Kaid MA, El-Sayed NZ, Ibrahim AA (2006) Physical properties of ZnO thin films deposited by spray pyrolysis technique. Appl Surf Sci 252(22):7844–7848. https://doi.org/10.1016/j.apsusc.2005.09.048

Badireddy AR, Wiesner MR, Liu J (2012) Detection, characterization, and abundance of engineered nanoparticles in complex waters by hyperspectral imagery with enhanced Darkfield microscopy. Environ Sci Technol 46(18):10081–10088. https://doi.org/10.1021/es204140s

Bai Y-X, Li Y-F, Yang Y, Yi L-X (2006) Covalent immobilization of triacylglycerol lipase onto functionalized novel mesoporous silica supports. J Biotechnol 125(4):574–582

Balasubramanian C, Joseph B, Gupta P, Saini NL, Mukherjee S, Di Gioacchino D, Marcelli A (2014) X-ray absorption spectroscopy characterization of iron-oxide nanoparticles synthesized

by high temperature plasma processing. J Electron Spectrosc Relat Phenom 196:125–129. https://doi.org/10.1016/j.elspec.2014.02.011

Begum R, Farooqi ZH, Naseem K, Ali F, Batool M, Xiao J, Irfan A (2018) Applications of UV/Vis spectroscopy in characterization and catalytic activity of noble metal nanoparticles fabricated in responsive polymer microgels: a review. Crit Rev Anal Chem 48(6):503–516

Berkmans J, Jagannatham M, Reddy R, Haridoss P (2015) Synthesis of thin bundled single walled carbon nanotubes and nanohorn hybrids by arc discharge technique in open air atmosphere. Diam Relat Mater 55:12–15

Bet-Moushoul E, Farhadi K, Mansourpanah Y, Nikbakht AM, Molaei R, Forough M (2016) Application of CaO-based/Au nanoparticles as heterogeneous nanocatalysts in biodiesel production. Fuel 164:119–127. https://doi.org/10.1016/j.fuel.2015.09.067

Binnig G, Rohrer H (1983) Scanning tunneling microscopy. Surf Sci 126(1–3):236–244

Bonaccorso F, Lombardo A, Hasan T, Sun Z, Colombo L, Ferrari AC (2012) Production and processing of graphene and 2d crystals. Mater Today 15(12):564–589. https://doi.org/10.1016/S1369-7021(13)70014-2

Bota P, Dorobantu D, Boerasu I, Bojin D, Enachescu M (2015) New laser ablation chamber for producing carbon nanomaterials using excimer laser. Mater Res Innov 19(1):33–39

Boz N, Degirmenbasi N, Kalyon DM (2009) Conversion of biomass to fuel: transesterification of vegetable oil to biodiesel using KF loaded nano-γ-Al_2O_3 as catalyst. Appl Catal B Environ 89(3–4):590–596

Carlsson J-O, Martin PM (2010) Chapter 7. Chemical vapor deposition. In: Martin PM (ed) Handbook of deposition technologies for films and coatings, 3rd edn. William Andrew Publishing, Boston, pp 314–363. https://doi.org/10.1016/B978-0-8155-2031-3.00007-7

Chen Z, Westerhoff P, Herckes P (2008a) Quantification of C60 fullerene concentrations in water. Environ Toxicol Chem 27(9):1852–1859

Chen YZ, Yang CT, Ching CB, Xu R (2008b) Immobilization of lipases on hydrophobilized zirconia nanoparticles: highly enantioselective and reusable biocatalysts. Langmuir 24(16):8877–8884

Choi S, Byeon C, Park D, Jeong M (2016) Polarization-selective alignment of a carbon nanotube film by using femtosecond laser ablation. J Korean Phys Soc 68(2):210–214

Chrzanowska J, Hoffman J, Małolepszy A, Mazurkiewicz M, Kowalewski TA, Szymanski Z, Stobinski L (2015) Synthesis of carbon nanotubes by the laser ablation method: effect of laser wavelength. Phys Status Solidi B 252(8):1860–1867

Cooper AJ, Wilson NR, Kinloch IA, Dryfe RA (2014) Single stage electrochemical exfoliation method for the production of few-layer graphene via intercalation of tetraalkylammonium cations. Carbon 66:340–350

Cui J, Björnmalm M, Ju Y, Caruso F (2018) Nanoengineering of poly(ethylene glycol) particles for stealth and targeting. Langmuir 34(37):10817–10827. https://doi.org/10.1021/acs.langmuir.8b02117

Dao ATN, Mott DM, Maenosono S (2015) Characterization of metallic nanoparticles based on the abundant usages of X-ray techniques. In: Handbook of nanoparticles, pp 1–24

de la Calle I, Menta M, Klein M, Séby F (2017) Screening of TiO_2 and Au nanoparticles in cosmetics and determination of elemental impurities by multiple techniques (DLS, SP-ICP-MS, ICP-MS and ICP-OES). Talanta 171:291–306. https://doi.org/10.1016/j.talanta.2017.05.002

Degueldre C, Favarger P-Y (2004) Thorium colloid analysis by single particle inductively coupled plasma-mass spectrometry. Talanta 62(5):1051–1054

Degueldre C, Favarger P-Y, Bitea C (2004) Zirconia colloid analysis by single particle inductively coupled plasma-mass spectrometry. Anal Chim Acta 518(1–2):137–142

Dobrucka R, Długaszewska J (2016) Biosynthesis and antibacterial activity of ZnO nanoparticles using Trifolium pratense flower extract. Saudi J Biol Sci 23(4):517–523. https://doi.org/10.1016/j.sjbs.2015.05.016

Du W, Xu Y, Liu D, Zeng J (2004) Comparative study on lipase-catalyzed transformation of soybean oil for biodiesel production with different acyl acceptors. J Mol Catal B Enzym 30(3–4):125–129

Dutta S, Ganguly BN (2012) Characterization of ZnO nanoparticles grown in presence of folic acid template. J Nanobiotechnol 10(1):29

Dyal A, Loos K, Noto M, Chang SW, Spagnoli C, Shafi KV, Ulman A, Cowman M, Gross RA (2003) Activity of *Candida rugosa* lipase immobilized on γ-Fe_2O_3 magnetic nanoparticles. J Am Chem Soc 125(7):1684–1685

Fang X, Shashurin A, Teel G, Keidar M (2016) Determining synthesis region of the single wall carbon nanotubes in arc plasma volume. Carbon 107:273–280

Firouzjaee MH, Taghizadeh M (2017) Optimization of process variables for biodiesel production using the nanomagnetic catalyst CaO/NaY-Fe_3O_4. Chem Eng Technol 40(6):1140–1148

Fischer HC, Fournier-Bidoz S, Chan W, Pang K (2007) Quantitative detection of engineered nanoparticles in tissues and organs: an investigation of efficacy and linear dynamic ranges using ICP-AES. NanoBiotechnology 3(1):46–54

Gao C, Zhai Y, Ding Y, Wu Q (2010) Application of sweet sorghum for biodiesel production by heterotrophic microalga Chlorella protothecoides. Appl Energy 87(3):756–761

Glatter O (2018) Chapter 11. Dynamic Light Scattering (DLS). In: Glatter O (ed) Scattering methods and their application in colloid and Interface science. Elsevier, Amsterdam, pp 223–263. https://doi.org/10.1016/B978-0-12-813580-8.00011-0

Goriparti S, Miele E, De Angelis F, Di Fabrizio E, Proietti Zaccaria R, Capiglia C (2014) Review on recent progress of nanostructured anode materials for Li-ion batteries. J Power Sources 257:421–443. https://doi.org/10.1016/j.jpowsour.2013.11.103

Guo J, Li J, Kou H (2011) Chapter 19. Chemical preparation of advanced ceramic materials. In: Xu R, Pang W, Huo Q (eds) Modern inorganic synthetic chemistry. Elsevier, Amsterdam, pp 429–454. https://doi.org/10.1016/B978-0-444-53599-3.10019-8

Han H, Guan Y (2009) Synthesis of biodiesel from rapeseed oil using K_2O/γ-Al_2O_3 as nano-solid-base catalyst. Wuhan Univ J Nat Sci 14(1):75–79

Hoo CM, Starostin N, West P, Mecartney ML (2008) A comparison of atomic force microscopy (AFM) and dynamic light scattering (DLS) methods to characterize nanoparticle size distributions. J Nanopart Res 10(1):89–96

Horak D, Babič M, Mackova H, Beneš MJ (2007) Preparation and properties of magnetic nano- and microsized particles for biological and environmental separations. J Sep Sci 30(11):1751–1772

Hou B, Wu C, Inoue T, Chiashi S, Xiang R, Maruyama S (2017) Extended alcohol catalytic chemical vapor deposition for efficient growth of single-walled carbon nanotubes thinner than (6,5). Carbon 119:502–510. https://doi.org/10.1016/j.carbon.2017.04.045

Hu S, Guan Y, Wang Y, Han H (2011) Nano-magnetic catalyst KF/CaO–Fe_3O_4 for biodiesel production. Appl Energy 88(8):2685–2690

Ionescu MI, Zhang Y, Li R, Sun X, Abou-Rachid H, Lussier L-S (2011) Hydrogen-free spray pyrolysis chemical vapor deposition method for the carbon nanotube growth: parametric studies. Appl Surf Sci 257(15):6843–6849

Jamdagni P, Khatri P, Rana JS (2018) Green synthesis of zinc oxide nanoparticles using flower extract of Nyctanthes arbor-tristis and their antifungal activity. J King Saud Univ Sci 30(2):168–175. https://doi.org/10.1016/j.jksus.2016.10.002

James AE, Driskell JD (2013) Monitoring gold nanoparticle conjugation and analysis of biomolecular binding with nanoparticle tracking analysis (NTA) and dynamic light scattering (DLS). Analyst 138(4):1212–1218

Ji X, Zhang W, Li X, Yu H, Dong H (2017) A novel hybrid method combining ASP with PECVD for in-situ low temperature synthesis of vertically aligned carbon nanotube films. Diam Relat Mater 77:16–24

Jin Y, Kannan S, Wu M, Zhao JX (2007) Toxicity of luminescent silica nanoparticles to living cells. Chem Res Toxicol 20(8):1126–1133

Kaur M, Ali A (2011) Lithium ion impregnated calcium oxide as nano catalyst for the biodiesel production from karanja and jatropha oils. Renew Energy 36(11):2866–2871

Khan I, Saeed K, Khan I (2017) Nanoparticles: properties, applications and toxicities. Arab J Chem. https://doi.org/10.1016/j.arabjc.2017.05.011

Kim HH, Kim HJ (2006) Preparation of carbon nanotubes by DC arc discharge process under reduced pressure in an air atmosphere. Mater Sci Eng B 133(1–3):241–244
Konwarh R, Karak N, Rai SK, Mukherjee AK (2009) Polymer-assisted iron oxide magnetic nanoparticle immobilized keratinase. Nanotechnology 20(22):225107
Kucinskis G, Bajars G, Kleperis J (2013) Graphene in lithium ion battery cathode materials: a review. J Power Sources 240:66–79. https://doi.org/10.1016/j.jpowsour.2013.03.160
Kwon SS, Jeon SH, Shon JK, Kim DH, Chang IS, Kim JM (2007) Preparation and stabilization of chitosan-lipase composite within mesoporous silica material. Solid State Phenom, Trans Tech Publ:1717–1720
Lee Y-C, Lee K, Oh Y-K (2015) Recent nanoparticle engineering advances in microalgal cultivation and harvesting processes of biodiesel production: a review. Bioresour Technol 184:63–72. https://doi.org/10.1016/j.biortech.2014.10.145
Li Y, Ruan Z, Zheng M, Deng Q, Zhang S, Zheng C, Tang H, Huang F, Shi J (2018) *Candida rugosa* lipase covalently immobilized on facilely-synthesized carbon nitride nanosheets as a novel biocatalyst. RSC Adv 8(26):14229–14236
Lin V, Mahoney P, Gibson K (2009) Nanofarming technology extracts biofuel oil without harming algae. News released from Office of Public Affairs
Liu X-M, Huang Z, Oh S, Zhang B, Ma P-C, Yuen MMF, Kim J-K (2012) Carbon nanotube (CNT)-based composites as electrode material for rechargeable Li-ion batteries: a review. Compos Sci Technol 72(2):121–144. https://doi.org/10.1016/j.compscitech.2011.11.019
Logeswari P, Silambarasan S, Abraham J (2015) Synthesis of silver nanoparticles using plants extract and analysis of their antimicrobial property. J Saudi Chem Soc 19(3):311–317. https://doi.org/10.1016/j.jscs.2012.04.007
López-Serrano A, Olivas RM, Landaluze JS, Cámara C (2014) Nanoparticles: a global vision. Characterization, separation, and quantification methods. Potential environmental and health impact. Anal Methods 6(1):38–56
Lu AH, Salabas EL, Schüth F (2007) Magnetic nanoparticles: synthesis, protection, functionalization, and application. Angew Chem Int Ed 46(8):1222–1244
Lu J, Yang J-x, Wang J, Lim A, Wang S, Loh KP (2009) One-pot synthesis of fluorescent carbon nanoribbons, nanoparticles, and graphene by the exfoliation of graphite in ionic liquids. ACS Nano 3(8):2367–2375. https://doi.org/10.1021/nn900546b
Luz Martínez S, Romero R, López JC, Romero A, Sánchez Mendieta VC, Natividad R (2010) Preparation and characterization of CaO nanoparticles/NaX zeolite catalysts for the transesterification of sunflower oil. Ind Eng Chem Res 50(5):2665–2670
Ma S, Livingstone R, Zhao B, Lombardi JR (2011) Enhanced Raman spectroscopy of nanostructured semiconductor phonon modes. J Phys Chem Lett 2(6):671–674
Madhuvilakku R, Piraman S (2013) Biodiesel synthesis by TiO_2–ZnO mixed oxide nanocatalyst catalyzed palm oil transesterification process. Bioresour Technol 150:55–59. https://doi.org/10.1016/j.biortech.2013.09.087
Magrez A, Kasas S, Salicio V, Pasquier N, Seo JW, Celio M, Catsicas S, Schwaller B, Forró L (2006) Cellular toxicity of carbon-based nanomaterials. Nano Lett 6(6):1121–1125
Marchand P, Hassan IA, Parkin IP, Carmalt CJ (2013) Aerosol-assisted delivery of precursors for chemical vapour deposition: expanding the scope of CVD for materials fabrication. Dalton Trans 42(26):9406–9422
Margulis-Goshen K, Magdassi S (2012) Organic nanoparticles from microemulsions: formation and applications. Curr Opin Colloid Interface Sci 17(5):290–296. https://doi.org/10.1016/j.cocis.2012.06.005
Maria KH, Mieno T (2015) Synthesis of single-walled carbon nanotubes by low-frequency bipolar pulsed arc discharge method. Vacuum 113:11–18. https://doi.org/10.1016/j.vacuum.2014.11.025
Maruyama S, Kojima R, Miyauchi Y, Chiashi S, Kohno M (2002) Low-temperature synthesis of high-purity single-walled carbon nanotubes from alcohol. Chem Phys Lett 360(3–4):229–234
Maruyama T, Kondo H, Ghosh R, Kozawa A, Naritsuka S, Iizumi Y, Okazaki T, Iijima S (2016) Single-walled carbon nanotube synthesis using Pt catalysts under low ethanol pres-

sure via cold-wall chemical vapor deposition in high vacuum. Carbon 96:6–13. https://doi.org/10.1016/j.carbon.2015.09.010

Matinise N, Fuku XG, Kaviyarasu K, Mayedwa N, Maaza M (2017) ZnO nanoparticles via Moringa oleifera green synthesis: physical properties & mechanism of formation. Appl Surf Sci 406:339–347. https://doi.org/10.1016/j.apsusc.2017.01.219

Meland H, Johannessen T, Arstad B, Venvik HJ, Rønning M, Holmen A (2006) Preparation of low temperature water-gas shift catalysts by flame spray pyrolysis. In: Gaigneaux EM, Devillers M, De Vos DE et al (eds) Studies in surface science and catalysis, vol 162. Elsevier, pp 985–992. https://doi.org/10.1016/S0167-2991(06)81006-2

Meysami SS, Dillon F, Koós AA, Aslam Z, Grobert N (2013a) Aerosol-assisted chemical vapour deposition synthesis of multi-wall carbon nanotubes: I. Mapping the reactor. Carbon 58:151–158

Meysami SS, Koós AA, Dillon F, Grobert N (2013b) Aerosol-assisted chemical vapour deposition synthesis of multi-wall carbon nanotubes: II. An analytical study. Carbon 58:159–169

Meysami SS, Koos AA, Dillon F, Dutta M, Grobert N (2015) Aerosol-assisted chemical vapour deposition synthesis of multi-wall carbon nanotubes: III. Towards upscaling. Carbon 88:148–156

Miura S, Yoshihara Y, Asaka M, Hasegawa K, Sugime H, Ota A, Oshima H, Noda S (2018) Millimeter-tall carbon nanotube arrays grown on aluminum substrates. Carbon 130:834–842. https://doi.org/10.1016/j.carbon.2018.01.075

Mokhena TC, Luyt AS (2017a) Electrospun alginate nanofibres impregnated with silver nanoparticles: preparation, morphology and antibacterial properties. Carbohydr Polym 165:304–312

Mokhena TC, Luyt AS (2017b) Development of multifunctional nano/ultrafiltration membrane based on a chitosan thin film on alginate electrospun nanofibres. J Clean Prod 156:470–479

Montero JM, Wilson K, Lee AF (2010) Cs promoted triglyceride transesterification over MgO nanocatalysts. Top Catal 53(11–12):737–745

Moreno-Vega A-I, Gomez-Quintero T, Nunez-Anita R-E, Acosta-Torres L-S, Castaño V (2012) Polymeric and ceramic nanoparticles in biomedical applications. J Nanotechnol 2012:1

Mottana A (2014) 1913–2013 – the centennial of X-ray absorption spectroscopy (XAS): evidences about a question still open. J Electron Spectrosc Relat Phenom 196:14–19. https://doi.org/10.1016/j.elspec.2013.12.004

Mtibe A, Mokhothu TH, John MJ, Mokhena TC, Mochane MJ (2018) Chapter 8. Fabrication and characterization of various engineered nanomaterials. In: Mustansar Hussain C (ed) Handbook of nanomaterials for industrial applications. Elsevier, Amsterdam, pp 151–171. https://doi.org/10.1016/B978-0-12-813351-4.00009-2

Mubarak N, Abdullah E, Jayakumar N, Sahu J (2014) An overview on methods for the production of carbon nanotubes. J Ind Eng Chem 20(4):1186–1197

Muehlethaler C, Leona M, Lombardi JR (2015) Review of surface enhanced Raman scattering applications in forensic science. Anal Chem 88(1):152–169

Nemade K (2014) Waghuley S (2014) synthesis of MgO nanoparticles by solvent mixed spray pyrolysis technique for optical investigation. Int J Met 2014:1

Netto CG, Andrade LH, Toma HE (2009) Enantioselective transesterification catalysis by *Candida antarctica* lipase immobilized on superparamagnetic nanoparticles. Tetrahedron Asymmetry 20(19):2299–2304

Noureddini H, Gao X, Philkana R (2005) Immobilized Pseudomonas cepacia lipase for biodiesel fuel production from soybean oil. Bioresour Technol 96(7):769–777

Novoselov KS, Geim AK, Morozov SV, Jiang D, Zhang Y, Dubonos SV, Grigorieva IV, Firsov AA (2004) Electric field effect in atomically thin carbon films. Science 306(5696):666–669

Okitsu K (2013) UV-vis spectroscopy for characterization of metal nanoparticles formed from reduction of metal ions during ultrasonic irradiation. In: UV-VIS and photoluminescence spectroscopy for nanomaterials characterization. Springer, Berlin, pp 151–177

Omraei M, Sheibani S, Sadrameli SM, Towfighi J (2013) Preparation of biodiesel using KOH-MWCNT catalysts: an optimization study. Ind Eng Chem Res 52(5):1829–1835. https://doi.org/10.1021/ie301418y

Patil PS (1999) Versatility of chemical spray pyrolysis technique. Mater Chem Phys 59(3):185–198. https://doi.org/10.1016/S0254-0584(99)00049-8

Pena MDPS, Gottipati A, Tahiliani S, Neu-Baker NM, Frame MD, Friedman AJ, Brenner SA (2016) Hyperspectral imaging of nanoparticles in biological samples: simultaneous visualization and elemental identification. Microsc Res Tech 79(5):349–358

Pizarro AVL, Park EY (2003) Lipase-catalyzed production of biodiesel fuel from vegetable oils contained in waste activated bleaching earth. Process Biochem 38(7):1077–1082

Ramos AP (2017) 4 - dynamic light scattering applied to nanoparticle characterization. In: Da Róz AL, Ferreira M, de Lima Leite F, Oliveira ON (eds) Nanocharacterization techniques. William Andrew Publishing, Oxford, pp 99–110. https://doi.org/10.1016/B978-0-323-49778-7.00004-7

Rolland JP, Maynor BW, Euliss LE, Exner AE, Denison GM, DeSimone JM (2005) Direct fabrication and harvesting of monodisperse, shape-specific nanobiomaterials. J Am Chem Soc 127(28):10096–10100. https://doi.org/10.1021/ja051977c

Romero G, Moya SE (2012) Chapter 4. Synthesis of organic nanoparticles. In: de la Fuente JM, Grazu V (eds) Frontiers of nanoscience, vol 4. Elsevier, Amsterdam, pp 115–141. https://doi.org/10.1016/B978-0-12-415769-9.00004-2

Scheffer A, Engelhard C, Sperling M, Buscher W (2008) ICP-MS as a new tool for the determination of gold nanoparticles in bioanalytical applications. Anal Bioanal Chem 390(1):249–252

Seo DJ, Cho MY, Park SB (2006) Preparation of titania nanoparticles of anatase phase by using flame spray pyrolysis. In: Rhee H-K, Nam I-S, Park JM (eds) Studies in surface science and catalysis, vol 159. Elsevier, Amsterdam, pp 761–764. https://doi.org/10.1016/S0167-2991(06)81708-8

Shah S, Solanki K, Gupta MN (2007) Enhancement of lipase activity in non-aqueous media upon immobilization on multi-walled carbon nanotubes. Chem Cent J 1(1):30

Shao Y, Wu C, Wu T, Yuan C, Chen S, Ding T, Ye X, Hu Y (2018) Green synthesis of sodium alginate-silver nanoparticles and their antibacterial activity. Int J Biol Macromol 111:1281–1292. https://doi.org/10.1016/j.ijbiomac.2018.01.012

Sigfridsson K, Björkman J-A, Skantze P, Zachrisson H (2011) Usefulness of a nanoparticle formulation to investigate some hemodynamic parameters of a poorly soluble compound. J Pharm Sci 100(6):2194–2202. https://doi.org/10.1002/jps.22440

Solanki K, Gupta M (2011) Simultaneous purification and immobilization of *Candida rugosa* lipase on superparamagnetic Fe_3O_4 nanoparticles for catalyzing transesterification reactions. New J Chem 35(11):2551–2556

Sree R, Babu NS, Prasad PS, Lingaiah N (2009) Transesterification of edible and non-edible oils over basic solid Mg/Zr catalysts. Fuel Process Technol 90(1):152–157

Su Y, Yang Z, Wei H, Kong ES-W, Zhang Y (2011) Synthesis of single-walled carbon nanotubes with selective diameter distributions using DC arc discharge under CO mixed atmosphere. Appl Surf Sci 257(7):3123–3127. https://doi.org/10.1016/j.apsusc.2010.10.127

Su Y, Wei H, Li T, Geng H, Zhang Y (2014) Low-cost synthesis of single-walled carbon nanotubes by low-pressure air arc discharge. Mater Res Bull 50:23–25. https://doi.org/10.1016/j.materresbull.2013.10.013

Tamilselvi P, Yelilarasi A, Hema M, Anbarasan R (2013) Synthesis of hierarchical structured MgO by sol-gel method. Nano Bulletin 2(1):130106

Tsang SC, Yu CH, Gao X, Tam K (2006) Silica-encapsulated nanomagnetic particle as a new recoverable biocatalyst carrier. J Phys Chem B 110(34):16914–16922

Ullah F, Nosheen A, Hussain I, Banon A (2009) Base catalyzed transesterification of wild apricot kernel oil for biodiesel production. Afr J Biotechnol 8(14)

van der Pol E, Coumans FAW, Sturk A, Nieuwland R, van Leeuwen TG (2014) Refractive index determination of nanoparticles in suspension using nanoparticle tracking analysis. Nano Lett 14(11):6195–6201. https://doi.org/10.1021/nl503371p

Vander Wal R, Berger G, Ticich T (2003) Carbon nanotube synthesis in a flame using laser ablation for in situ catalyst generation. Appl Phys A 77(7):885–889

Venkat Reddy CR, Oshel R, Verkade JG (2006) Room-temperature conversion of soybean oil and poultry fat to biodiesel catalyzed by nanocrystalline calcium oxides. Energy Fuel 20(3):1310–1314

Verziu M, Cojocaru B, Hu J, Richards R, Ciuculescu C, Filip P, Parvulescu VI (2008) Sunflower and rapeseed oil transesterification to biodiesel over different nanocrystalline MgO catalysts. Green Chem 10(4):373–381

Vicente G, Bautista LF, Rodríguez R, Gutiérrez FJ, Sádaba I, Ruiz-Vázquez RM, Torres-Martínez S, Garre V (2009) Biodiesel production from biomass of an oleaginous fungus. Biochem Eng J 48(1):22–27

Wang J-T (2011) Chapter 7. CVD and its related theories in inorganic synthesis and materials preparations. In: Xu R, Pang W, Huo Q (eds) Modern inorganic synthetic chemistry. Elsevier, Amsterdam, pp 151–171. https://doi.org/10.1016/B978-0-444-53599-3.10007-1

Wang L, Yang J (2007) Transesterification of soybean oil with nano-MgO or not in supercritical and subcritical methanol. Fuel 86(3):328–333

Wang Y, Hu S-y, Guan Y-p, Wen L-b, Han H-y (2009) Preparation of mesoporous nanosized KF/CaO–MgO catalyst and its application for biodiesel production by transesterification. Catal Lett 131(3–4):574–578

Wen L, Wang Y, Lu D, Hu S, Han H (2010) Preparation of KF/CaO nanocatalyst and its application in biodiesel production from Chinese tallow seed oil. Fuel 89(9):2267–2271

Williams DN, Ehrman SH, Holoman TRP (2006) Evaluation of the microbial growth response to inorganic nanoparticles. J Nanobiotechnol 4(1):3

Xiang B, Wang P, Zhang X, Dayeh SA, Aplin DPR, Soci C, Yu D, Wang D (2007) Rational synthesis of p-type zinc oxide nanowire arrays using simple chemical vapor deposition. Nano Lett 7(2):323–328. https://doi.org/10.1021/nl062410c

Xie W, Ma N (2009) Immobilized lipase on Fe_3O_4 nanoparticles as biocatalyst for biodiesel production. Energy Fuel 23(3):1347–1353

Xu H, Miao X, Wu Q (2006) High quality biodiesel production from a microalga Chlorella protothecoides by heterotrophic growth in fermenters. J Biotechnol 126(4):499–507

Yacob AR, Mustajab M, Samadi NS (2009) Calcination temperature of nano MgO effect on base transesterification of palm oil. World Acad Sci Eng Technol 56:408–412

Yang G, Tian-Wei T, Kai-Li N, Fang W (2006) Immobilization of lipase on macroporous resin and its application in synthesis of biodiesel in low aqueous media. Chin J Biotechnol 22(1):114–118

Yu J, Yu X (2008) Hydrothermal synthesis and photocatalytic activity of zinc oxide hollow spheres. Environ Sci Technol 42(13):4902–4907. https://doi.org/10.1021/es800036n

Yu J, Wang W, Cheng B, Su B-L (2009) Enhancement of photocatalytic activity of Mesporous TiO2 powders by hydrothermal surface fluorination treatment. J Phys Chem C 113(16):6743–6750. https://doi.org/10.1021/jp900136q

Zhang XL, Yan S, Tyagi RD, Surampalli RY (2013) Biodiesel production from heterotrophic microalgae through transesterification and nanotechnology application in the production. Renew Sust Energ Rev 26:216–223. https://doi.org/10.1016/j.rser.2013.05.061

Zhao X, Ohkohchi M, Inoue S, Suzuki T, Kadoya T, Ando Y (2006) Large-scale purification of single-wall carbon nanotubes prepared by electric arc discharge. Diam Relat Mater 15(4–8):1098–1102

Zhao J, Wei L, Yang Z, Zhang Y (2012) Continuous and low-cost synthesis of high-quality multi-walled carbon nanotubes by arc discharge in air. Physica E 44(7):1639–1643. https://doi.org/10.1016/j.physe.2012.04.010

Zhong YL, Swager TM (2012) Enhanced electrochemical expansion of graphite for in situ electrochemical functionalization. J Am Chem Soc 134(43):17896–17899

Zhou C, Krueger AB, Barnard JG, Qi W, Carpenter JF (2015) Characterization of nanoparticle tracking analysis for quantification and sizing of submicron particles of therapeutic proteins. J Pharm Sci 104(8):2441–2450. https://doi.org/10.1002/jps.24510